EUSAR 2021 . ISBN 978-3-8007-5457-1 / ISSN 2197-4403 . ©VDE VERLAG GMBH . Berlin . Offenbach

A Model-Free Ratio based Nonlocal Framework for Denoising of SAR and TomoSAR data

H. Aghababaei[a], R. Zamani[b] G. Ferraioli[c], V. Pascazio[d], G. Schirinzi[d]
[a] Faculty of Geo-Information Science and Earth Observation (ITC), Department of Earth Observation Science (EOS), University of Twente, Enschede, the Netherlands.
[b] Faculty of Geodesy and geomatic engineering, K.N. Toosi University of technology, Tehran, Iran.
[c]Dipartimento di Ingegneria, Università degli Studi di Napoli "Parthenope," Napoli, Italy
[d] Dipartimento di Scienze e Tecnologie, Università degli Studi di Napoli "Parthenope", Napoli, Italy

Abstract

This paper introduces a general patch-based model-free framework for despeckling of single and multi-baseline synthetic aperture radar (SAR) image. Particularly, the method is based on the empirical distribution similarity between the patch containing the pixel to be restored and the patch containing a candidate similar pixel. In order to decide whether the patches follow a similar distribution, the Kolmogorov–Smirnov test is adapted. Finally, within the restoration process, the selected similar pixels are aggregated based on their relative importance obtained according to their distribution similarities. Experimental validation of the proposed methodology is provided using different real data sets and compared with existing NLSAR approach in relation to single SAR image despeckling and tomographic application for the 3D reflectivity reconstruction of volumetric media as well as permanent scatterer detection in urban environments.

1 Introduction

The coherent synthetic aperture radar (SAR) images are affected by the well-known multiplicative speckle noise [1]. The speckle may increase the intensity fluctuations and severely diminish the performance of information extraction techniques in single SAR image as well as in the applications requiring multi-baseline SAR tomography (TomoSAR) data sets. Accordingly, the despeckling as a preprocessing step is often an imperative task in order to fully exploit the SAR images for different applications.

The attempts for designing efficient despeckling filter is a long-standing research topic and a general review of existing frameworks can be found in [2]. From the different existing speckle reduction techniques, a boosted performance in terms of denoising and resolution preserving has been reported in the literature with the framework of non-local (NL) or patch-based filtering approaches [3]. The first contribution of NL techniques for SAR image restoration and despeckling back to the study of reference [4] in 2000. The basic principle of NL filter is moving from local neighboring pixels to non-local similar pixel and restoring pixel value by exploiting similar pixels in the image, where those usually detected by a searching window around the selected pixel. It is known that the weighted averaging of similar pixels can effectively suppress the speckle with perceptible preservation of structures and the textures. However, the most critical aspect of NL approaches returns to the decision of choosing similar pixel. This is mainly performed through a similarity or dissimilarity criterion, where it quantifies how much the two specific patches are similar or different. It is undetectable that the similarity between two patches can be defined as the sum of the similarity of each pair of corresponding pixels in the two noisy patches in the image. Then, if two noisy patches are similar according to the defined criteria, then the central pixels of the patches are used together in the filtering process.

In the last years, several criterions have been proposed and evaluated for computing the (di) similarity of noisy patches. From different existing criterions including information-based, geometric-based and detection-based frameworks, the generalized likelihood ratio (GLR) criterion is shown to be one the most significant technique. For more information about the different criterions, the reader may refer to the works in [3, 5].
However, the developed criterions in the literature mainly rely on a fundamental Goodman's fully developed speckle model, where it may not be held in high-resolution images of man-made environments, in which persistent scatterers and not fully developed speckle are frequently encountered. In such a case, when the estimated criterion accounts for the particular speckle model, the efficiency of NL based filtering can be severely impaired.
Hence, the model-free approaches of comparing noisy patches that is sorely lacking in the literature would be very useful.
In this paper, a model-free NL based algorithm able to work with multi-channel images is presented. A variety of SAR products from a single image to polarimetric, and interferometric SAR data can be processed. The proposed framework is based on the estimation of two similarity criteria, one obtained by direct comparison of the patches distributions, while the other compares the distribution of the ratio patches. Generally, if the two patches are similar, it is expected that both ratio and the inverse ratio being indicative of speckles ratio will follow the same distribution. The model-free approach allows avoiding a wrong characterization of the speckle model: the algorithm will

EUSAR 2021 . ISBN 978-3-8007-5457-1 / ISSN 2197-4403 . ©VDE VERLAG GMBH . Berlin . Offenbach

not force any statistical hypothesis for all possible scenarios: homogeneous, heterogeneous, extremely heterogeneous areas, or mixed. At the same time, the algorithm will benefit of the NL paradigm, providing effective results both in terms of speckle reduction and details preservation.

The next Section presents the proposed non-local filtering framework for single and multi-baseline SAR images.

2 Proposed Approach

2.1 The proposed similarity measure for the case of single channel SAR Image

This sub-section presents the proposed similarity measure in single channel SAR images, while the next sub-section presents it for multi-channel cases.

Having a single channel SAR image, the information of a patch P can be represented with the amplitudes (or intensities) of K related pixels:

$$\mathbf{a}(P)=[A(p_1)\ \ A(p_2)\ \ ....\ \ A(p_K)] \qquad (1)$$

where A(p_i) denotes the amplitude of i^{th} pixel in the patch P. In general, the vector **a**(P) may follow the random model for the distributed targets, where no dominant scatterer is presented; while for a point-like scatterer **a**(P) is a K-dimensional deterministic vector. However, without concern about the distribution of the patch information, two given noisy patches P and Q can be compared. Particularly, the *Null hypothesis* that two patches are similar can be approved if: 1) the vectors **a**(P) and **a**(Q are drawn from the same statistical distribution. 2) The ratio vector **v**=**a**(P)/**a**(Q) and its element-wise reciprocal **v**.$^{-1}$ are drawn from same statistical distribution.

It is readily understandable that in the alternative hypothesis, the previous statements are not valid and neither **a**(P) and **a**(Q) nor **v** and **v**$^{-1}$follow the same distributions, since the deterministic parts of the patches are different. Hence, the proposed similarity criteria for single-channel SAR image is defined based on the distance between the distributions that can be measured using the KS distances as:

$$\begin{aligned}\delta_{\mathbf{a}} &= \max|E_{\mathbf{a}P}-E_{\mathbf{aQ}}|(\sqrt{K}+0.12+0.11/\sqrt{K})\\ \delta_{\mathbf{v}} &= \max|E_{\mathbf{v}P}-E_{\mathbf{vQ}}|(\sqrt{K}+0.12+0.11/\sqrt{K})\end{aligned} \qquad (2)$$

Where $E_{\mathbf{a}\mathrm{P}}$ and $E_{\mathbf{a}\mathrm{P}}$ represent the ECDFs of **a**(P) and **a**(Q), while $E_{\mathbf{v}\mathrm{P}}$ and $E_{\mathbf{v}\mathrm{P}}$ indicate the ECDFs of **v** and **v**.$^{-1}$, respectively. It should be noted that the term $\sqrt{K}+0.12+0.11/\sqrt{K}$ in (2) is adapted to extricate the dependence of KS distance to the considered patch size.

2.2 The proposed similarity measure for the case of multi-channel SAR data

In a general case, let us refer to a stack of N co-registered SLC SAR images, where the scattering vector of a pixel p is represented by $\mathbf{y}(p)\epsilon\mathbb{C}^{N\times 1}$. It is being understood that in case of fully polarimetric data set, the complex entries of **y**(p) corresponds to each combination of emission/reception polarizations. Under the reciprocity theorem, the emission and reception of electromagnet signal with horizontal(h)/vertical(v) polarizations leads to representation of scattering vector as $\mathbf{y}(p)=[\mathbf{y}_{\mathrm{HH}}\ \mathbf{y}_{\mathrm{HV}}\ \mathbf{y}_{\mathrm{VV}}]^{\mathrm{T}}\epsilon\mathbb{C}^{3\times 1}$. In addition, **y**($p$)may encounter the stack of backscattering from multi-channel images constructed by interferometric (InSAR) data or even polarimetric interferometric (PolInSAR) data modalities.

The use of pre-estimated sample covariance matrix is a straightforward way to represent multi-look multi-channel information of pixels. The pre-estimated covariance matrix can be computed using L limited neighborhood pixels as:

$$\hat{\mathbf{C}}=\sum_{l=1}^{L} y(l)y^{\dagger}(l) \qquad (3)$$

where † is the Hermitian operator.

To represent the information of a patch P in multi-channel data set, the informative vector can be defined as:

$$\mathbf{a}(P)=[tr(\hat{\mathbf{C}}(p_1))\ \ tr(\hat{\mathbf{C}}(p_2))\ \ ....\ \ tr(\hat{\mathbf{C}}(p_K))] \qquad (4)$$

where tr(.) is the trace operator. Needless to point out that for single-channel SAR image Eq. (4) boils down to intensity vector in (1).

Considering the multiplicative characteristic of speckle, the fluctuation in multi-channel SAR images can be modeled using the following relation between sample $\hat{\mathbf{C}}$and true[redacted]covariance matrices, *i.e.*

$$\hat{\mathbf{C}}=\mathbf{\Sigma}^{1/2}\mathbf{S}\mathbf{\Sigma}^{1/2} \qquad (5)$$

where $\mathbf{S}$ = E{$\mathbf{ss}^{\dagger}$} and $\mathbf{s}$ =[s_1 s_2 ... s_N]$^{\mathrm{T}}$ indicates the speckle component of multi-channel target vector. Following the relation in (5), let define the ratio and inverse ratio matrices between two pre-estimated sample covariance matrices as:

$$\begin{aligned}\mathbf{X}_{p,q} &= \hat{\mathbf{C}}(q)^{-1/2}\hat{\mathbf{C}}(p)\hat{\mathbf{C}}(q)^{-1/2}\\ \mathbf{X}_{q,p} &= \hat{\mathbf{C}}(p)^{-1/2}\hat{\mathbf{C}}(q)\hat{\mathbf{C}}(p)^{-1/2}\end{aligned} \qquad (6)$$

From (5), when the true covariance matrices of the pixels are equal, i.e. $\mathbf{\Sigma}(p)=\mathbf{\Sigma}(q)$, then the sample covariance becomes characterized by only speckle. Thus, in these conditions, both **X**(p,q) and **X**(q,p) will correspond to the ratio between speckle matrices. In such a case, it is expected that the traces of **X**(p,q) and **X**(q,p) follow the same distribution model. From this fact the ratio vector **v** in multi-channel case is defined as:

$$\begin{aligned}\mathbf{v} &= [tr(\mathbf{X}_{q_1,p_1})\ \ tr(\mathbf{X}_{q_2,p_2}) \ldots.. tr(\mathbf{X}_{q_K,p_K})]\\ \mathbf{v}.^{-1} &= [tr(\mathbf{X}_{p_1,q_1})\ \ tr(\mathbf{X}_{p_2,q_2}) \ldots.. tr(\mathbf{X}_{p_K,q_K})]\end{aligned} \qquad (7)$$

Accordingly, in analogy to the single-channel denoising framework, when two patches P and Q are similar, the *Null hypothesis* cannot be disapproved if: 1) the vectors **a**(P) and **a**(Q) in are drawn from the same statistical distribution. 2) The ratio and inverse ratio vectors (**v** and **v**$^{-1}$ are drawn from the same statistical distribution.

Giving the vector **a** and **v**, the KS distances represented in (2) can be computed. Once the similarity distances are computed, the next step can be proceeded in order to map the similarities into a weight function.

EUSAR 2021 . ISBN 978-3-8007-5457-1 / ISSN 2197-4403 . ©VDE VERLAG GMBH . Berlin . Offenbach

2.3 Aggregation process.

In contrast to local despeckling techniques, the nonlocal approaches do not select essentially the neighborhood pixels, but rather samples that most likely follow the same distribution within an extended neighborhood. Hence, for a reference pixel p the extended neighborhood can be defined by a search window that constructed around the pixel. Then, from the previously described method, the similarity of each pixel in the search window to the reference pixel is computed. Once the similarity of the samples in the extended neighborhood has been computed, it is mandatory to define how to aggregate these samples in order to have a NL estimation of the restored pixel. For this aim, the weighting function has to be defined according to the relative importance of each sample used in the NL estimation. In the proposed despeckling approach, the weights are derived from the probability distribution of KS distances in (2), when the null hypothesis is approved. The weight functions for both KS distances are reported in Figure 1. It should be noted that the plots are representing the PDFs of the KS distances of two noisy patches, whose deterministic components are equal.

From both PDFs, it is apparent that pixels with small values of the KS distances are considered within the fusion step, while pixels belonging to patches having large distances are neglected. The final weight function for the aggregation of the pixels can be defined as:

$$w(p,q) = \sqrt{w_a(p,q)w_v(p,q)} \quad (8)$$

where w_a and w_v are the weight function related to KS distances δ_a and δ_v, respectively (See Figure 1).

Once the similarities are mapped into a weight value using (8), the nonlocal covariance matrix is computed using the weighted maximum likelihood estimator as:

$$\hat{\mathbf{R}}(p) = \frac{\sum_q w(p,q)\hat{\mathbf{C}}(q)}{\sum_q w(p,q)} \quad (8)$$

3 Experiments

3.1 Single Channel experiment

In this subsection, the evaluation of the proposed approach with the single-channel amplitude SAR image is provided. The evaluations have been conducted on the images of Tehran study areas, obtained by TerraSAR-X image in HH polarization channel. To evaluate the proposed techniques, results of different filtering approaches namely, Noland [6], refined Lee[7], and NLSAR[8] are reported. For quantitative analysis, in addition to the ratio image, the statistical quality index (SQI) proposed in [9] is considered.

In Figure 2, the results of employed filtering approaches for the amplitude image of the test site (Azadi stadium in Tehran) are shown. From the visual comparison, the restored image by NLSAR is affected by over-smoothing effect in homogeneous regions (upper right of Figure 2 d).

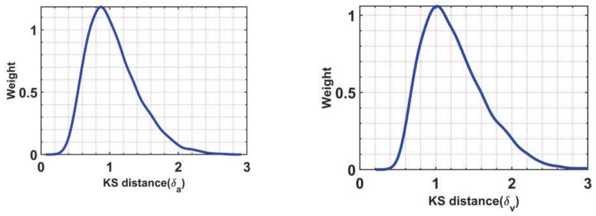

(a) (b)

Figure 1. Weighting functions for the proposed algorithm in case of 5-look three channels data set.

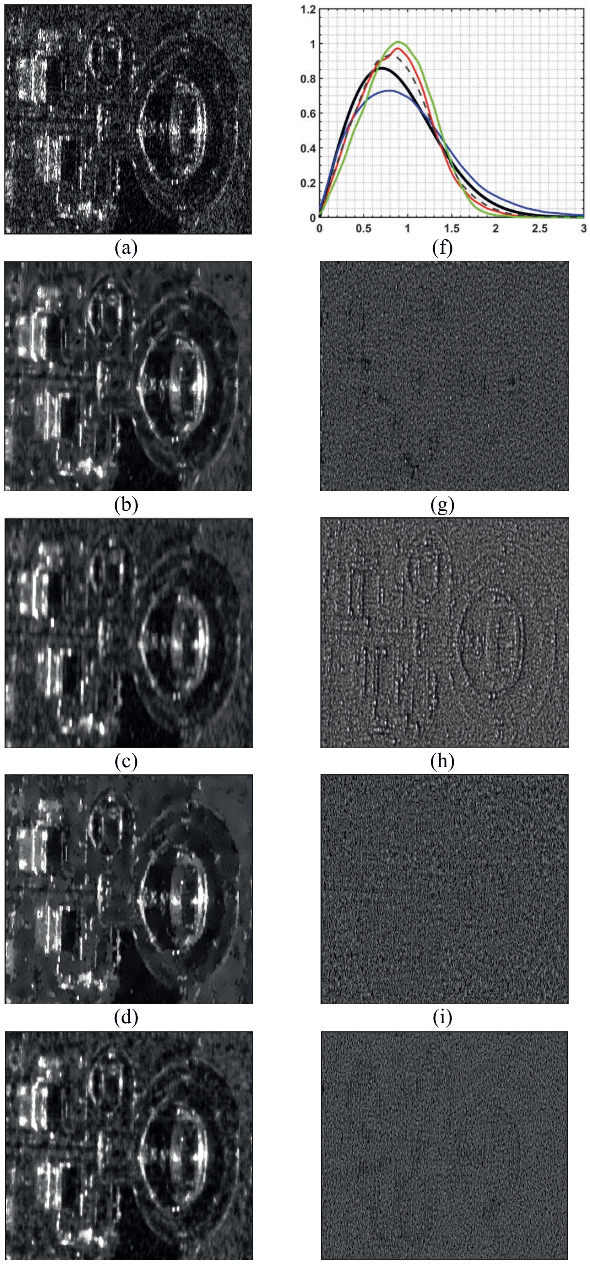

(a) (f) (b) (g) (c) (h) (d) (i) (e) (j)

Single channel despeckling operations on Tehran test site. First column: the original and filtered image. (a) original SLC amplitude image, (b) Noland, (c) refined Lee, (d) NLSAR, (e) the proposed method. The second column: the ratio image and the related PDFs. (f) Overlapping of the theoretical PDFs (black solid line) and of the ratio amplitude images. The ratio images by (g) Noland, (h) refined Lee, (i) NLSAR, and (j) the proposed method. In the PDF plot image, dash gray, blue, red, and green are related to Noland, refined Lee, NLSAR, and the proposed method, respectively.

EUSAR 2021 . ISBN 978-3-8007-5457-1 / ISSN 2197-4403 . ©VDE VERLAG GMBH . Berlin . Offenbach

In the results by proposed method, Noland and refined Lee, this issue is correctly addressed (Figure 2. b, c and e). For further evaluation, the ratio images are estimated and illustrated in the second column of Figure 2. Generally, with an ideal filter, only speckle should remain in the ratio image. In the ratio images produced by refined Lee structures are visible. Moreover, some spot structures are remained in the ratio image of Noland (Figure 2 g) due to some over-smoothing in building areas. Approximately, the same structures, with some additional details are visible in the proposed solution. Although in the ratio image by the NLSAR (Figure2 i) the structures and the contents are less remained, its filtered image sufferers, as said before, from over-smoothing effect.

3.2 Polarimetric SAR experiment

After assessing the method on single-channel amplitude images, further evaluation is conducted on fully polarimetric data sets. The results are compared with IDAN[10], refined Lee and NLSAR approaches. To this aim, the despeckled polarimetric covariance matrix of the Oberpfaffenhofen test sites, provided by DLR's ESAR sensor at L band, are estimated using the employed approaches. The qualitative evaluation again is performed using the visual inspection on the obtained filtered and the ratio images presented in Pauli color-coded.

Figure 3 reports the restored and ratio image of the Oberpfaffenhofen area in the Pauli basis coloring. Visual comparison of the filtered images with respect to the original one in Figure 3(a) affirms that the proposed method outperforms the others, both in terms of speckle removal and details preservation. Moreover, in order to verify it, the ratio covariance matrix (or speckle matrix) of each method is estimated using $\hat{\mathbf{S}} = \mathbf{\Sigma}^{-1/2}\hat{\mathbf{C}}\mathbf{\Sigma}^{-1/2}$ and their correspond Pauli ratio images are shown in the second column of Figure 3. As mentioned before, with effective filtering only speckle should remain in the ratio image. As can be noticed in Figure 3 (e) and (f), the structures remain in the ratio images derived from the IDAN and refined Lee, which indicates the poor performance of despeckling filtering. Although NLSAR decreases the geometric contents in the ratio image (Figure 3 i), most pixels are not properly filtered, where the restored image (Figure 3 d) is still affected by the noise effect. Instead, in the output of the proposed approach (Figure 3 e) the noise effect is notably reduced, while the edges are preserved (Figure 3 j). The ratio image appears characterized by limited details and an almost homogeneously distributed residual speckle.

It should be noted that further experimental results from multi-baseline tomographic data will be provided in the conference.

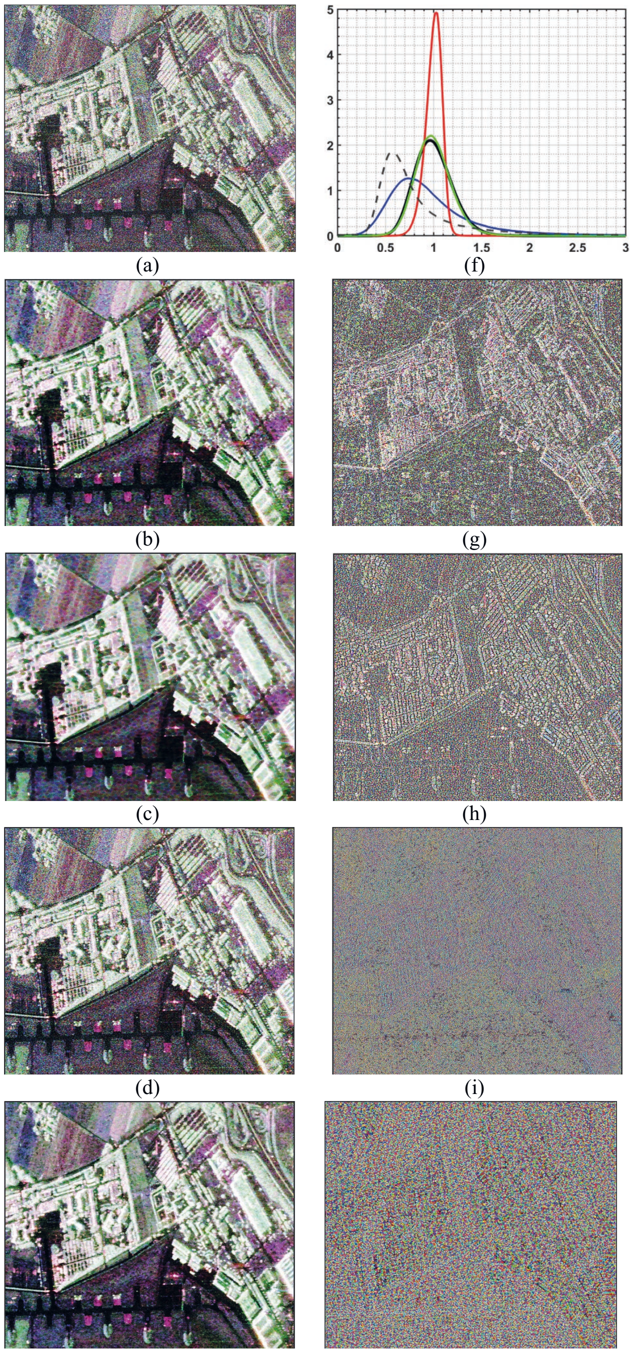

Results of filtering operations in Pauli basis representation of Oberpfaffenhofen test site. First column: the original and filtered image. (a) original image, (b) IDAN, (c) refined Lee, (d) NLSAR, (e) the proposed method. The second column: the ratio image and the related PDFs. (f) Overlapping of the theoretical PDFs (black solid line) and of the ratio amplitude images. The ratio images by (g) IDAN, (h) refined Lee, (i) NLSAR, and (j) the proposed method. In the PDF plot image, dash gray, blue, red, and green are related to IDAN, refined Lee, NLSAR, and the proposed method, respectively.

Literature

[1] J. W. Goodman, "Some fundamental properties of speckle*," *J. Opt. Soc. Am.*, vol. 66, no. 11,

EUSAR 2021 . ISBN 978-3-8007-5457-1 / ISSN 2197-4403 . ©VDE VERLAG GMBH . Berlin . Offenbach

pp. 1145-1150, 1976/11/01 1976, doi: 10.1364/JOSA.66.001145.

[2] F. Argenti, A. Lapini, T. Bianchi, and L. Alparone, "A Tutorial on Speckle Reduction in Synthetic Aperture Radar Images," *IEEE Geoscience and Remote Sensing Magazine,* vol. 1, no. 3, pp. 6-35, 2013, doi: 10.1109/MGRS.2013.2277512.

[3] C. Deledalle, L. Denis, G. Poggi, F. Tupin, and L. Verdoliva, "Exploiting Patch Similarity for SAR Image Processing: The nonlocal paradigm," *IEEE Signal Processing Magazine,* vol. 31, no. 4, pp. 69-78, 2014, doi: 10.1109/MSP.2014.2311305.

[4] A. Buades, B. Coll, and J.-M. Morel, "A review of image denoising algorithms, with a new one," *Multiscale Modeling & Simulation,* vol. 4, no. 2, pp. 490-530, 2005.

[5] C.-A. Deledalle, L. Denis, and F. Tupin, "How to compare noisy patches? Patch similarity beyond Gaussian noise," *International journal of computer vision,* vol. 99, no. 1, pp. 86-102, 2012.

[6] G. Ferraioli, V. Pascazio, and G. Schirinzi, "Ratio-Based Nonlocal Anisotropic Despeckling Approach for SAR Images," *IEEE Transactions on Geoscience and Remote Sensing,* vol. 57, no. 10, pp. 7785-7798, 2019, doi: 10.1109/TGRS.2019.2916465.

[7] J.-S. Lee, "Refined filtering of image noise using local statistics," *Computer graphics and image processing,* vol. 15, no. 4, pp. 380-389, 1981.

[8] C. Deledalle, L. Denis, F. Tupin, A. Reigber, and M. Jäger, "NL-SAR: A Unified Nonlocal Framework for Resolution-Preserving (Pol)(In)SAR Denoising," *IEEE Transactions on Geoscience and Remote Sensing,* vol. 53, no. 4, pp. 2021-2038, 2015, doi: 10.1109/TGRS.2014.2352555.

[9] H. Aghababaei and G. Ferraioli, "Statistical Indices for Despeckling Evaluation in Multichannel SAR Images," *IEEE geoscience and remote sensing letters,* 2020.

[10] G. Vasile, E. Trouvé, J.-S. Lee, and V. Buzuloiu, "Intensity-driven adaptive-neighborhood technique for polarimetric and interferometric SAR parameters estimation," *IEEE Transactions on Geoscience and Remote Sensing,* vol. 44, no. 6, pp. 1609-1621, 2006.